



# 1 Regional-scale lateral carbon transport and CO<sub>2</sub> evasion in 2 temperate stream catchments

3

4 Katrin Magin<sup>1</sup>, Celia Somlai-Haase<sup>1</sup>, Ralf B. Schäfer<sup>1</sup> and Andreas Lorke<sup>1</sup>

5 <sup>1</sup>Institute for Environmental Sciences, University of Koblenz-Landau, Fortstr. 7, D-76829 Landau, Germany

6 Correspondence to: Katrin Magin (magi6618@uni-landau.de)

7

8

9 **Abstract.** Inland waters play an important role in regional to global scale carbon cycling by transporting, processing  
10 and emitting substantial amounts of carbon, which originate mainly from their catchments. In this study, we  
11 analyzed the relationship between terrestrial net primary production (NPP) and the rate at which carbon is exported  
12 from the catchments in a temperate stream network. The analysis included more than 200 catchment areas in  
13 southwest Germany, ranging in size from 0.8 to 889 km<sup>2</sup> for which CO<sub>2</sub> evasion from stream surfaces and  
14 downstream transport with stream discharge were estimated from water quality monitoring data, while NPP in the  
15 catchments was obtained from a global data set based on remote sensing. We found that on average 2.7 % of  
16 terrestrial NPP (13.9 g C m<sup>2</sup> yr<sup>-1</sup>) are exported from the catchments by streams and rivers, in which both CO<sub>2</sub>  
17 evasion and downstream transport contributed about equally to this flux. The average carbon fluxes in the  
18 catchments of the study area resembled global and large-scale zonal mean values in many respects, including NPP,  
19 stream evasion as well as the catchment-specific total export rate of carbon in the fluvial network. A review of  
20 existing studies on aquatic-terrestrial coupling in the carbon cycle suggests that the catchment-specific carbon export  
21 varies in a relatively narrow range, despite a broad range of different spatial scales and hydrological characteristics  
22 of the study regions.

## 23 **Keywords**

24 Regional carbon cycle, terrestrial-aquatic coupling, net primary production, CO<sub>2</sub> degassing from streams, land use



## 25 1 Introduction

26 Inland waters represent an important component of the global carbon cycle by transporting, storing and processing  
27 significant amounts of organic and inorganic carbon (C) and by emitting substantial amounts of carbon dioxide  
28 (CO<sub>2</sub>) to the atmosphere (Cole et al., 2007;Aufdenkampe et al., 2011). Globally about 0.32 to 0.8 Pg C is emitted per  
29 year as CO<sub>2</sub> from lakes and reservoirs (Raymond et al., 2013;Barros et al., 2011). For streams and rivers the global  
30 estimates range from 0.35 to 1.8 Pg C yr<sup>-1</sup> (Raymond et al., 2013;Cole et al., 2007), where the lower estimates can  
31 be considered as conservative because they omit CO<sub>2</sub> emissions from small headwater streams. Comparable  
32 amounts of carbon are discharged into the oceans by the world's rivers (0.9 Pg C yr<sup>-1</sup>) and stored in aquatic  
33 sediments (0.6 Pg C yr<sup>-1</sup>) (Tranvik et al., 2009). In total, evasion, discharge and storage of C in inland waters have  
34 been estimated to account for about 4 % of global terrestrial net primary production (NPP) (Raymond et al., 2013) or  
35 50-70 % of the total terrestrial net ecosystem production (NEP) (Cole et al., 2007). A recent continental-scale  
36 analysis, which combined terrestrial productivity estimates from a suite of biogeochemical models with estimates of  
37 the total aquatic C yield for the conterminous United States (Butman et al., 2015), resulted in mean C export rates  
38 from terrestrial into freshwater systems of 4 % of NPP and 27 % of NEP. These estimates varied by a factor of four  
39 across 18 hydrological units with surface areas between 10<sup>5</sup> and 10<sup>6</sup> km<sup>2</sup>.

40 The substantial lateral and vertical transport of terrestrial-derived C in inland waters is currently not accounted for in  
41 most bottom-up estimates of the terrestrial uptake rate of atmospheric CO<sub>2</sub> (Battin et al., 2009) and results in high  
42 uncertainties in regional-scale C budgets and predictions of their response to climate change, land use and water  
43 management. Only few studies have quantified C fluxes and pools including inland waters at the regional-scale  
44 ( $O(10^3-10^4 \text{ km}^2)$ ) (Christensen et al., 2007;Buffam et al., 2011;Jonsson et al., 2007;Maberly et al., 2013) or for small  
45 ( $O(1-10 \text{ km}^2)$ ) catchments (Leach et al., 2016;Shibata et al., 2005;Billett et al., 2004). The majority of existing  
46 regional-scale studies on terrestrial-aquatic C fluxes are from the boreal zone and are characterized by a relatively  
47 large fractional surface area covered by inland waters, a high abundance of lakes and high fluvial loads of dissolved  
48 organic carbon (DOC). Landscapes in the temperate zone can differ in all these aspects, potentially resulting in  
49 differences in the relative importance of aquatic C-fluxes and flux paths (storage, evasion and discharge) in regional-  
50 scale C budgets differ. In this study, we analyzed the relationship between terrestrial NPP and CO<sub>2</sub> evasion and C  
51 discharge for more than 200 catchments in southwest Germany. The stream-dominated catchments range in size  
52 from 0.8 to 889 km<sup>2</sup> and are characterized by a relatively small fraction of surface water coverage (< 0.5 % of the  
53 land surface area). In contrast to studies from the boreal zone, the fluvial C load is dominated by dissolved inorganic  
54 carbon (DIC). Estimates of aquatic C export from the catchments were obtained from water quality and hydrological  
55 monitoring data and were related to terrestrial NPP derived from MODIS satellite data. The scale dependence of  
56 aquatic carbon fluxes in relation to NPP is analyzed by grouping the data according to stream order. By comparing  
57 our results to a variety of published studies, we finally discuss the magnitude as well as the relative importance of  
58 different fluvial flux paths in regional-scale C budgets in different landscapes and climatic zones.



## 59 2 Materials and Methods

### 60 2.1 Study area and hydrological characteristics

61 The study area encompasses large parts of the federal state of Rhineland-Palatinate (RLP) in southwest Germany  
62 (Fig. 1). The average altitude is 323 m (48 m - 803 m) and the mean annual temperature and precipitation varied  
63 between 5.8 and 12.2 °C and 244 and 1576 mm during the time period between 1991 and 2011 at the 37  
64 meteorological stations operated by the state RLP (<http://www.wetter.rlp.de/>). The dominating land cover in the  
65 study area is woodland (41 %, mainly mixed and broad-leaved forest), tilled land (37 %, mainly arable land and  
66 vineyards) and grassland (13 %, mainly pastures) (Corine land cover (EEA, 2006)).

67 Most of the rivers in RLP are part of the catchment area of the Rhine River. Other large rivers in the state are Mosel,  
68 Lahn, Saar and Nahe. The upland regions of RLP are sources to many small, steep and highly turbulent streams with  
69 gravel beds (MULEWF, 2015). Lakes in RLP are small with a total area of approximately 40 km<sup>2</sup> (Statistisches  
70 Landesamt Rheinland-Pfalz, 2014) and were omitted from the analysis. The river network has a total length of 15  
71 800 km and consists of stream orders (Strahler, 1957) between 1 and 7 order. A catchment map of RLP, consisting  
72 of subcatchments of 7729 river segments was provided by the state ministry (MULEWF, 2013), where a river  
73 segment refers to the section between a source and the first junction with another river or between two junctions  
74 with other rivers. All subsequent analyses were conducted separately for each stream order and streams of Strahler  
75 order >4 were omitted from the analysis because of the limited sample size with only few catchments available.  
76 Moreover, we omitted streams for which parts of the catchment area were outside of the study area. Overall, 3377,  
77 1619, 861 and 453 stream segments were remaining for the analysis for Strahler order 1 to 4, respectively. Annual  
78 mean discharge and length of the river segments were obtained from digital maps provided by the state ministry  
79 (MULEWF, 2013).

### 80 2.2 Aquatic carbon concentrations

81 DIC concentrations and partial pressure of dissolved CO<sub>2</sub> ( $p\text{CO}_2$ ) in stream water were estimated from governmental  
82 water quality monitoring data. The data include measurements of alkalinity, pH and temperature which were  
83 conducted between 1977 and 2011 (MULEWF, 2013). Sampling intervals differed between the sites and water  
84 sampling was conducted irregularly with respect to year and season. To exclude a potential bias resulting from the  
85 seasonality of DIC concentrations on the analysis, we only considered river segments for which at least one  
86 measurement was available for each season (spring, summer, autumn, winter). From these measurements,  $p\text{CO}_2$  and  
87 DIC concentrations were estimated using chemical equilibrium calculations with the software PHREEQC (Version  
88 2) (Parkhurst and Appelo, 1999). For 201 river segments with seasonally resolved measurements, we first computed  
89 seasonal mean  $p\text{CO}_2$  and DIC concentrations, which subsequently were aggregated to annual mean values averaged  
90 over the entire sampling period. Measurements of dissolved and total organic C (DOC, TOC) were available only  
91 for 54 of these sampling sites.



### 92 2.3 Estimation of lateral DIC export and catchment-scale CO<sub>2</sub> evasion

93 The lateral export of DIC and the total CO<sub>2</sub> evasion from the upstream located stream network was calculated for  
 94 each of the 201 sampling sites with seasonally averaged concentration estimates. Lateral DIC export from the  
 95 corresponding catchments was calculated as the product of the mean DIC concentration and discharge. CO<sub>2</sub> evasion  
 96 from the stream network upstream of each sampling site was estimated by interpolating *p*CO<sub>2</sub> for all river segments  
 97 without direct measurements. For this, the mean concentrations were averaged by stream order and assigned to all  
 98 stream segments of the river network (Butman and Raymond, 2011). Stream width (*w*, in m), depth (*d*, in m) and  
 99 flow velocity (*v*, in m s<sup>-1</sup>) were estimated from the discharge (*Q*, in m<sup>3</sup> s<sup>-1</sup>) using the following empirical equations  
 100 (Leopold and Maddock Jr, 1953):

$$101 \quad w = a * Q^b \quad d = c * Q^d \quad v = e * Q^f, \quad (1)$$

102 For the hydraulic geometry exponents and coefficients, the values from Raymond et al. (2012) were used (*b*=0.29,  
 103 *d*=0.42, *f*=0.29, *a*=0.4, *c*=12.88 and *e*=0.19).

104 The water surface area (*A*, in m<sup>2</sup>) was calculated as the product of length and width of the river segments. The  
 105 average slope for each segment was estimated from a Digital Elevation Map (resolution 10 m) provided by the  
 106 federal state of Rhineland-Palatinate (LVerGeoRP, 2012). The gas transfer velocity of CO<sub>2</sub> at 20°C (*k*<sub>600</sub>, in m d<sup>-1</sup>)  
 107 was calculated from slope (*S*) and flow velocity (*v*, in m s<sup>-1</sup>) (Raymond et al., 2012).

$$108 \quad k_{600} = S * v * 2841.6 + 2.03 \quad (2)$$

109 This gas transfer velocity was adjusted to the in situ temperature (*k*<sub>*T*</sub>, in m d<sup>-1</sup>) using the following equation:

$$110 \quad k_T = k_{600} * \left( \frac{Sc_T}{600} \right)^{-0.5}, \quad (3)$$

111 where *Sc*<sub>*T*</sub> is the Schmidt number (ratio of the kinematic viscosity of water and the diffusion coefficient of dissolved  
 112 CO<sub>2</sub>) at the in situ temperature (Raymond et al., 2012). Finally the CO<sub>2</sub> flux (*F*<sub>*D*</sub>, in g C m<sup>-2</sup> yr<sup>-1</sup>) for each stream  
 113 segment was calculated as:

$$114 \quad F_D = k_T * K_H (pCO_2 - pCO_{2,a}) * M_C \quad (4)$$

115 The partial pressure of CO<sub>2</sub> in the atmosphere (*p*CO<sub>2,*a*</sub>) was considered as constant (390 ppm) and the Henry  
 116 coefficient of CO<sub>2</sub> at in-situ temperature (*K*<sub>*H*</sub> in mol l<sup>-1</sup> atm<sup>-1</sup>) was estimated using the relationship provided in  
 117 (Stumm and Morgan, 1996). *M*<sub>*C*</sub> is the molar mass of C (12 g mol<sup>-1</sup>). Finally, the total CO<sub>2</sub> evasion was estimated by  
 118 summing up the product of *F*<sub>*D*</sub> with the corresponding water surface area for all stream segments located upstream  
 119 of each individual sampling point.

### 120 2.4 Estimation of the catchment NPP

121 Average NPP in the catchment areas of the study sites were obtained from a global data set derived from moderate  
 122 resolution imaging spectroradiometer (MODIS) observations of the earth observing system (EOS) satellites, which  
 123 is available for the time period 2000 to 2013 with a spatial resolution of 30 arc seconds (~ 1 km<sup>2</sup>) (Zhao et al., 2005).  
 124 In this data set, NPP was estimated based on remote sensing observations of spectral reflectance, land cover and



125 surface meteorology as described in detail by Running et al. (2004). We used mean NPP data (2000-2013) averaged  
126 over the catchment areas of the individual sampling sites.

## 127 **2.5 Statistical analysis**

128 Linear regressions (F-test) were used to analyze the data. Group differences or correlations with  $p < 0.05$  were  
129 considered statistically significant. For the regression of total aquatic C export rate and annual catchment NPP, data  
130 were log-transformed to correct for normal distribution.

## 131 **3 Results**

### 132 **3.1 Catchment characteristics and aquatic C load**

133 The size of the analyzed catchment areas varied over three orders of magnitude (0.8 to 889 km<sup>2</sup>) and the mean size  
134 increased from 9 km<sup>2</sup> for 1<sup>st</sup> order streams to 243 km<sup>2</sup> for streams of the order 4 (Table 1). Mean discharge and  
135 catchment area were linearly correlated ( $r^2 = 0.74$ ,  $p < 0.001$ ). The drainage rate, i.e. the stream discharge divided by  
136 the catchment area, was relatively constant across stream orders with a mean value of 0.28 m y<sup>-1</sup>, corresponding to  
137 35 % of the annual mean precipitation rate in the study area. The mean discharge increased more than 30-fold from  
138 0.06 to 2.2 m<sup>3</sup> s<sup>-1</sup> for 1<sup>st</sup> to 4<sup>th</sup> order streams, respectively. Similarly, the estimated water surface area increased with  
139 increasing stream order from 0.24 to 0.42 % of the corresponding catchment size (Table 1).

140 Individual estimates of the CO<sub>2</sub> partial pressure at the sampling sites varied between 145 and 7759 ppm. Only 1 %  
141 of the  $p\text{CO}_2$  values were below the mean atmospheric value (390 ppm), indicating that the majority of the stream  
142 network was a source of atmospheric CO<sub>2</sub> at all seasons. The total mean value of  $p\text{CO}_2$  was 2083 ppm and  $p\text{CO}_2$  and  
143 DIC did not differ significantly among the different stream orders ( $p\text{CO}_2$ :  $p = 0.35$ ; DIC:  $p = 0.56$ ).

144

145 The few available samples of DOC and TOC indicate that the organic C concentration was about one order of  
146 magnitude smaller than the inorganic C concentration (Table 1). Only a small fraction of TOC was in particulate  
147 form and TOC was linearly related to DIC, indicating that the organic load made up only 4 % of the total carbon  
148 load at the sampling sites (Fig. 2).

### 149 **3.2 Catchment NPP and C budget**

150 NPP increased linearly with catchment size ( $r^2 = 0.98$ ,  $p < 0.001$ ), but the specific NPP, i.e. the total NPP within a  
151 catchment divided by catchment area, did not differ significantly ( $p = 0.24$ ) among catchments of different stream  
152 orders. The smallest mean value and the largest variability (mean±sd: 466±127 g C m<sup>-2</sup> yr<sup>-1</sup>, range: 106 to 661 g C  
153 m<sup>-2</sup> yr<sup>-1</sup>) was observed among the small catchments of 1<sup>st</sup> order streams, while the variability was consistently  
154 smaller for higher stream orders (Table 2). The total average of terrestrial NPP in the study area was 515±79 g C m<sup>-2</sup>  
155 yr<sup>-1</sup> (mean±sd).



156 In a simplified catchment-scale C balance, we consider the sum of the DIC discharge (DIC concentration multiplied  
157 by discharge) measured at each sampling site and the total CO<sub>2</sub> evasion from the upstream located stream network  
158 as the total amount of C that is exported from the catchment area through the aquatic conduit. The total evasion was  
159 estimated by interpolation with stream-order specific *p*CO<sub>2</sub> values assigned to the complete stream network. Given  
160 the small number of available measurements, we neglect the fraction of organic C which is exported with stream  
161 discharge. As demonstrated above, TOC load is small in comparison to the DIC load (Fig. 2), resulting in a  
162 comparably small (< 4 %) error.

163 The resulting CO<sub>2</sub> evasion rates decreased slightly, but not significantly (*p*=0.26) for increasing stream orders with a  
164 total mean evasion rate of 2032 g C m<sup>-2</sup> yr<sup>-1</sup> (expressed as per unit water surface area) (Table 2). The total aquatic  
165 evasion rate within catchments normalized by the size of the catchment increased significantly with stream order  
166 with a mean value of 6.6 g C m<sup>-2</sup> yr<sup>-1</sup>. (Table 2).

167 The total aquatic C export rate, i.e. the sum of evasion and DIC discharge, was strongly correlated with annual mean  
168 NPP averaged over the corresponding catchment area. Linear regression of the log-transformed data results in a  
169 power-law exponent of 1.06, indicating a nearly linear relationship (Fig. 3). Most of the correlation between both  
170 quantities, however, can be attributed to their common linear scale-dependence.

171

172 After normalization with catchment area, the total aquatic C export rate increased slightly with stream order (Fig.  
173 4a). Also the fraction of NPP which was exported through the aquatic network, i.e. the sum of evasion and  
174 discharge, increased slightly, though not significantly (*p*=0.32), from 2.18 % for first-order stream to 2.72 % for  
175 stream order 4 (Fig. 4b). This increase was related to increasing rates of CO<sub>2</sub> evasion in streams of higher order and  
176 the contribution of evasion to the total C export rate increased from 39 to 53 % (Fig. 4c). The increasing evasion is  
177 mainly caused by the increasing fractional water surface area for increasing stream orders (Table 1), because the  
178 CO<sub>2</sub> fluxes per water surface showed a rather opposing trend with decreasing fluxes for increasing stream orders  
179 (Table 2). On average 1.31 % of the catchment NPP are emitted as CO<sub>2</sub> from the stream network and 1.49 % are  
180 discharged downstream (Table 2).

181

182 No regional (large-scale) pattern or gradients were observed in the spatial variation of catchment-scale NPP and  
183 aquatic C export (Fig. 5).

## 184 **4 Discussion**

### 185 **4.1. An average study region**

186 The average carbon fluxes in the catchments of the study area resemble global and large-scale zonal mean estimates  
187 in many aspects. The mean atmospheric flux of CO<sub>2</sub> from the stream network of 2031±1527 g C m<sup>-2</sup> yr<sup>-1</sup> is in close  
188 agreement with bulk estimates for streams and rivers in the temperate zone of 2630 (Aufdenkampe et al., 2011) and



189 2370 g C m<sup>-2</sup> yr<sup>-1</sup> (Butman and Raymond, 2011). The fractional surface coverage of streams and rivers (0.42 % for  
190 stream order 4) corresponds to the global average of 0.47 % (Raymond et al., 2013) and also mean terrestrial NPP in  
191 the catchments (515 g C m<sup>-2</sup> yr<sup>-1</sup>) was in close correspondence to recent global mean estimates (495 g C m<sup>-2</sup> yr<sup>-1</sup>  
192 (Zhao et al., 2005)).

193 By combining CO<sub>2</sub> evasion and downstream C-export by stream discharge, we estimated that 2.7 % of terrestrial  
194 NPP (13.9 g C m<sup>-2</sup> yr<sup>-1</sup>) are exported from the catchments by streams and rivers, in which both evasion and discharge  
195 contributed equally to this flux. Also these findings are in close agreement with global and continental scale  
196 estimates, of 16 and 13.5 g C m<sup>-2</sup> yr<sup>-1</sup>, respectively (Table 3).

#### 197 **4.1. Aquatic C export across spatial scales**

198 Though not exhaustive, Table 3 provides data from a large share of existing studies relating the aquatic C export to  
199 terrestrial production in the corresponding catchments which cover a broad range of spatial scales and different  
200 landscapes. Except for the tropical forest of the Amazon basin, the aquatic carbon export normalized to catchment  
201 area estimated for temperate streams in our study, is surprisingly similar to those estimated at comparable and at  
202 larger spatial scale. In the Amazon, the fraction of terrestrial production that is exported by the fluvial network is  
203 more than twofold higher (nearly 7 % of NPP (Richey et al., 2002)). However, that a large fraction of the regional  
204 NPP in the Amazon is supported by aquatic primary production by macrophytes and carbon export is predominantly  
205 controlled by wetland connectivity (Abril et al., 2013), with wetlands covering up to 16 % of the land surface area.  
206 An additional peculiarity of the Amazon is, that in contrast to the remaining systems, the vast majority (87 %) of the  
207 total C export is governed by CO<sub>2</sub> evasion (Table 3), whereas lateral export constitutes a much smaller component.  
208 An exceptionally low fraction of NPP that is exported from aquatic systems at larger scale was estimated for the  
209 English Lake District (1.6 % (Maberly et al., 2013)), though only CO<sub>2</sub> evasion from lake surfaces was considered,  
210 i.e. downstream discharge by rivers was ignored. Their estimate agrees reasonably well with the fraction of  
211 catchment NPP that was emitted to the atmosphere from the stream network in the present study (1.3 %). If a similar  
212 share of catchment NPP was exported with river discharge also in the Lake District, the average mass of C exported  
213 from the aquatic systems per unit catchment area would be in close agreement with our and other larger-scale  
214 estimates (Table 3).

215 In more detailed studies at smaller scales and for individual catchments, aquatic C export was exclusively related to  
216 net ecosystem exchange (NEE) measured by eddy covariance. Here the estimated fractions of aquatic export range  
217 between 2 % of NEE in a temperate forest catchment (only discharge, evasion not considered, (Shibata et al., 2005))  
218 and 160 % of NEE in a boreal peatland catchment (Billett et al., 2004). Analysis of inter-annual variations of stream  
219 export from a small peatland catchment in Sweden (Leach et al., 2016) resulted in estimates of C export by the  
220 fluvial network between 5.9 and 18.1 g C m<sup>-2</sup> yr<sup>-1</sup> over 12 years. The total mean value of 12.2 g C m<sup>-2</sup> yr<sup>-1</sup>, however,  
221 is in close agreement with the present and other larger-scale estimates (Table 3). In contrast to the present study, C  
222 export from the peatland catchments were dominated by stream discharge of dissolved organic carbon.



#### 223 4.2 Controlling factors for aquatic C export

224 We found a significant linear relationship between total catchment NPP and the C export from the catchment in the  
225 stream network across four Strahler orders. The relationship was mainly caused by a strong correlation between  
226 catchment size and water surface area. As expected, large streams and rivers with large surface area have larger  
227 catchments. A study analyzing aquatic carbon fluxes for 18 hydrological units in the conterminous U.S. (Butman et  
228 al., 2015) observed a significant correlation between catchment-specific aquatic C yield and specific catchment  
229 NEP, which in turn was linearly correlated to NPP. We did not observe such correlation at smaller scale, which  
230 could be related to the rather narrow range of variability in NPP among the considered catchments. Nevertheless, the  
231 linear correlation observed by (Butman et al., 2015) indicates that a constant fraction of terrestrial NPP is exported  
232 by aquatic systems if averaged over larger spatial scales.

233 The relatively narrow range of variability of C export per catchment area (between 9 and 18 g C m<sup>2</sup> yr<sup>-1</sup>, with the  
234 two exceptions discussed above) in different landscapes (Table 3) is rather surprising. Although this range of  
235 variation is most likely within the uncertainty of the various estimates, the variability across different landscapes is  
236 certainly small in comparison to the order of magnitude differences in potential controlling factors. In lake-rich  
237 regions, evasion from inland waters was observed to be dominated by lakes (Buffam et al., 2011;Jonsson et al.,  
238 2007), which cover up to 13 % of the surface area. In the present as well as in other studies on catchments where  
239 lakes are virtually absent (Wallin et al., 2013) and the fractional water coverage was smaller than 0.5 % of the  
240 terrestrial surface area, an almost identical catchment-specific C export and evasion rate has been observed (Table  
241 3). CO<sub>2</sub> emissions from water surfaces depend on the partial pressure of CO<sub>2</sub> in water and are therefore related to  
242 DIC, which was the dominant form of dissolved C in the present study. Studies in the boreal zone, where dissolved  
243 C in the aquatic systems is mainly in the form of DOC, however, found comparable catchment-specific C export and  
244 evasion rates ((Leach et al., 2016;Jonsson et al., 2007;Wallin et al., 2013), cf. Table 3). The difference in the  
245 speciation of the exported C indicates that a larger fraction of the terrestrial NPP is respired by heterotrophic  
246 respiration in soils and exported to the stream network as DIC in the present study, in contrast to export as DOC and  
247 predominantly aquatic respiration. Observations and modeling of terrestrial-aquatic C fluxes across the U.S.  
248 suggested a transition of the source of aquatic CO<sub>2</sub> from direct terrestrial input to aquatic CO<sub>2</sub> production by  
249 degradation of terrestrial organic carbon with increasing stream size (Hotchkiss et al., 2015). Such transition was not  
250 observed in the present study, where organic carbon made a small contribution to the fluvial carbon load across all  
251 investigated stream orders.

252 Despite the small number of observations, the narrow range of variability of C export per catchment area may  
253 indicate that neither water surface area nor the location of mineralization of terrestrial derived C (soil respiration and  
254 export of DIC versus export of DOC and mineralization in the aquatic environment), are important drivers for the  
255 total C export from catchments by inland waters at larger spatial scales. This rather unexpected finding deserves  
256 further attention, as it suggests that other, currently poorly explored, processes control the aquatic-terrestrial  
257 coupling and the role of inland waters in regional C cycling. Given the significant contribution of inland waters to  
258 regional and global scale greenhouse gas emissions, the mechanistic understanding of these processes is urgently





259 required to assess their vulnerability to ongoing climatic and land use changes, as well to the extensive  
260 anthropogenic influences on freshwater ecosystems. Recent developments of process-based models, which are  
261 capable of resolving the boundless biogeochemical cycle in the terrestrial–aquatic continuum from catchment to  
262 continental scales (Nakayama, 2016), are certainly an important tool for these future studies.

### 263 **Acknowledgments**

264 This study was financially supported by the German Research Foundation (grant no. LO 1150/9-1). We thank  
265 Miriam Tenhaken for contributing to a preliminary analysis. All raw data for this paper is properly cited and referred  
266 to in the reference list. The processed data, which were used to generate the figures and tables, are available upon  
267 request through the corresponding author.

268 **References**

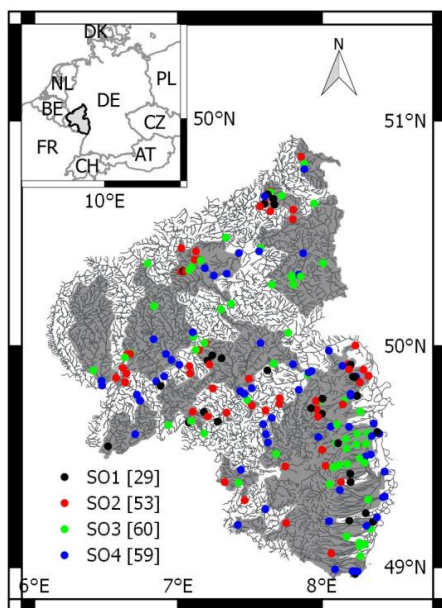
- 269 Abril, G., Martinez, J.-M., Artigas, L. F., Moreira-Turcq, P., Benedetti, M. F., Vidal, L., Meziane, T., Kim, J.-H.,  
 270 Bernardes, M. C., Savoye, N., Deborde, J., Souza, E. L., Alberic, P., Landim de Souza, M. F., and Roland, F.:  
 271 Amazon River carbon dioxide outgassing fuelled by wetlands, *Nature*, 505, 395-398, 10.1038/nature12797, 2013.
- 272 Aufdenkampe, A. K., Mayorga, E., Raymond, P. A., Melack, J. M., Doney, S. C., Alin, S. R., Aalto, R. E., and Yoo,  
 273 K.: Riverine coupling of biogeochemical cycles between land, oceans, and atmosphere, *Front. Ecol. Environ.*, 9, 53-  
 274 60, 10.1890/100014, 2011.
- 275 Barros, N., Cole, J. J., Tranvik, L. J., Prairie, Y. T., Bastviken, D., Huszar, V. L. M., del Giorgio, P., and Roland, F.:  
 276 Carbon emission from hydroelectric reservoirs linked to reservoir age and latitude, *Nature Geosci.*, 4, 593-596,  
 277 10.1038/ngeo1211, 2011.
- 278 Battin, T. J., Luysaert, S., Kaplan, L. A., Aufdenkampe, A. K., Richter, A., and Tranvik, L. J.: The boundless  
 279 carbon cycle, *Nature Geosci.*, 2, 598-600, 10.1038/ngeo618, 2009.
- 280 Billett, M. F., Palmer, S. M., Hope, D., Deacon, C., Storeton-West, R., Hargreaves, K. J., Flechard, C., and Fowler,  
 281 D.: Linking land-atmosphere-stream carbon fluxes in a lowland peatland system, *Global Biogeochem. Cycles*, 18,  
 282 n/a-n/a, 10.1029/2003GB002058, 2004.
- 283 Buffam, I., Turner, M. G., Desai, A. R., Hanson, P. C., Rusak, J. A., Lottig, N. R., Stanley, E. H., and Carpenter, S.  
 284 R.: Integrating aquatic and terrestrial components to construct a complete carbon budget for a north temperate lake  
 285 district, *Global Change Biol.*, 17, 1193-1211, 10.1111/j.1365-2486.2010.02313.x, 2011.
- 286 Butman, D., and Raymond, P. A.: Significant efflux of carbon dioxide from streams and rivers in the United States,  
 287 *Nature Geosci.*, 4, 839-842, 2011.
- 288 Butman, D., Stackpole, S., Stets, E., McDonald, C. P., Clow, D. W., and Striegl, R. G.: Aquatic carbon cycling in  
 289 the conterminous United States and implications for terrestrial carbon accounting, *Proceedings of the National*  
 290 *Academy of Sciences*, 10.1073/pnas.1512651112, 2015.
- 291 Christensen, T. R., Johansson, T., Olsrud, M., Ström, L., Lindroth, A., Mastepanov, M., Malmer, N., Friborg, T.,  
 292 Crill, P., and Callaghan, T. V.: A catchment-scale carbon and greenhouse gas budget of a subarctic landscape,  
 293 *Philosophical Transactions of the Royal Society of London A: Mathematical, Physical and Engineering Sciences*,  
 294 365, 1643-1656, 10.1098/rsta.2007.2035, 2007.
- 295 Cole, J. J., Prairie, Y. T., Caraco, N. F., McDowell, W. H., Tranvik, L. J., Striegl, R. G., Duarte, C. M., Kortelainen,  
 296 P., Downing, J. A., Middelburg, J. J., and Melack, J.: Plumbing the global carbon cycle: Integrating inland waters  
 297 into the terrestrial carbon budget, *Ecosystems*, 10, 171-184, 10.1007/s10021-006-9013-8, 2007.
- 298 EEA: Corine Land Cover 2006 seamless vector data, European Environment Agency, 2006.



- 299 Hotchkiss, E. R., Hall Jr, R. O., Sponseller, R. A., Butman, D., Klaminder, J., Laudon, H., Rosvall, M., and  
300 Karlsson, J.: Sources of and processes controlling CO<sub>2</sub> emissions change with the size of streams and rivers, *Nature*  
301 *Geosci.*, 8, 696-699, 10.1038/ngeo2507, 2015.
- 302 Jonsson, A., Algesten, G., Bergström, A. K., Bishop, K., Sobek, S., Tranvik, L. J., and Jansson, M.: Integrating  
303 aquatic carbon fluxes in a boreal catchment carbon budget, *J. Hydrol.*, 334, 141-150, 10.1016/j.jhydrol.2006.10.003,  
304 2007.
- 305 Leach, J. A., Larsson, A., Wallin, M. B., Nilsson, M. B., and Laudon, H.: Twelve year interannual and seasonal  
306 variability of stream carbon export from a boreal peatland catchment, *J. Geophys. Res.-Biogeo.*, 121, 1851-1866,  
307 10.1002/2016JG003357, 2016.
- 308 Leopold, L. B., and Maddock Jr, T.: The hydraulic geometry of stream channels and some physiographic  
309 implications 2330-7102, 1953.
- 310 L VermGeoRP: Vermessungs- und Katasterverwaltung Rheinland-Pfalz, Landesamt für Vermessung und  
311 Geobasisinformation Rheinland-Pfalz, 2012.
- 312 Maberly, S. C., Barker, P. A., Stott, A. W., and De Ville, M. M.: Catchment productivity controls CO<sub>2</sub> emissions  
313 from lakes, *Nature Climate Change*, 3, 391-394, 10.1038/nclimate1748, 2013.
- 314 MULEWF: GeoPortal Wasser, Ministerium für Umwelt, Landwirtschaft, Ernährung, Weinbau und Forsten  
315 Rheinland-Pfalz, 2013.
- 316 MULEWF: Wasserwirtschaftsverwaltung Rheinland-Pfalz, Ministerium für Umwelt, Landwirtschaft, Ernährung,  
317 Weinbau und Forsten Rheinland-Pfalz, 2015.
- 318 Nakayama, T.: New perspective for eco-hydrology model to constrain missing role of inland waters on boundless  
319 biogeochemical cycle in terrestrial-aquatic continuum, *Ecohydrology & Hydrobiology*, 16, 138-148,  
320 10.1016/j.ecohyd.2016.07.002, 2016.
- 321 Parkhurst, D. L., and Appelo, C.: User's guide to PHREEQC (Version 2): A computer program for speciation, batch-  
322 reaction, one-dimensional transport, and inverse geochemical calculations, 1999.
- 323 Ran, L., Lu, X. X., Yang, H., Li, L., Yu, R., Sun, H., and Han, J.: CO<sub>2</sub> outgassing from the Yellow River network  
324 and its implications for riverine carbon cycle, *J. Geophys. Res.-Biogeo.*, 120, 1334-1347, 10.1002/2015JG002982,  
325 2015.
- 326 Randerson, J. T., Chapin, F. S., Harden, J. W., Neff, J. C., and Harmon, M. E.: Net ecosystem production: a  
327 comprehensive measure of net carbon accumulation by ecosystems, *Ecol. Applications*, 12, 937-947, 10.1890/1051-  
328 0761(2002)012[0937:NEPACM]2.0.CO;2, 2002.



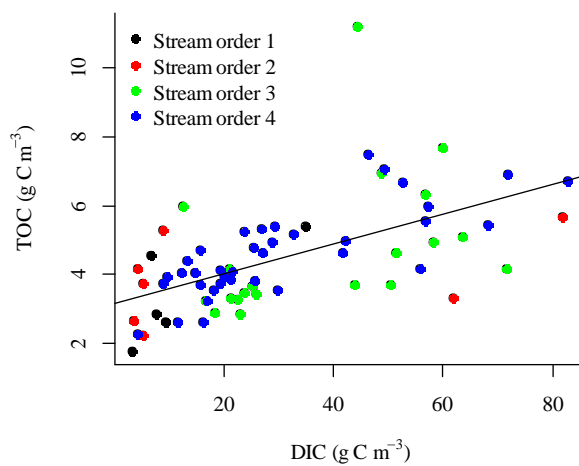
- 329 Raymond, P. A., Zappa, C. J., Butman, D., Bott, T. L., Potter, J., Mulholland, P., Laursen, A. E., McDowell, W. H.,  
 330 and Newbold, D.: Scaling the gas transfer velocity and hydraulic geometry in streams and small rivers, *Limnology*  
 331 and *Oceanography: Fluids and Environments*, 2, 41-53, 2012.
- 332 Raymond, P. A., Hartmann, J., Lauerwald, R., Sobek, S., McDonald, C., Hoover, M., Butman, D., Striegl, R.,  
 333 Mayorga, E., Humborg, C., Kortelainen, P., Durr, H., Meybeck, M., Ciais, P., and Guth, P.: Global carbon dioxide  
 334 emissions from inland waters, *Nature*, 503, 355-359, 10.1038/nature12760, 2013.
- 335 Richey, J. E., Melack, J. M., Aufdenkampe, A. K., Ballester, V. M., and Hess, L. L.: Outgassing from Amazonian  
 336 rivers and wetlands as a large tropical source of atmospheric CO<sub>2</sub>, *Nature*, 416, 617-620, 10.1038/416617a, 2002.
- 337 Running, S. W., Nemani, R. R., Heinsch, F. A., Zhao, M., Reeves, M., and Hashimoto, H.: A Continuous Satellite-  
 338 Derived Measure of Global Terrestrial Primary Production, *Bioscience*, 54, 547-560, 10.1641/0006-  
 339 3568(2004)054[0547:acsmog]2.0.co;2, 2004.
- 340 Sabine, C. L., Heimann, M., Artaxo, P., Bakker, D. C., Chen, C.-T. A., Field, C. B., Gruber, N., Le Quééré, C., Prinn,  
 341 R. G., and Richey, J. E.: Current status and past trends of the global carbon cycle, in: *The Global Carbon Cycle*, 2nd  
 342 ed., edited by: Field, C. B., and Raupach, M. R., Scientific Committee on Problems of the Environment (SCOPE)  
 343 Series, Island Press, 17-44, 2004.
- 344 Shibata, H., Hiura, T., Tanaka, Y., Takagi, K., and Koike, T.: Carbon cycling and budget in a forested basin of  
 345 southwestern Hokkaido, northern Japan, *Ecological Research*, 20, 325-331, 10.1007/s11284-005-0048-7, 2005.
- 346 Statistisches Landesamt Rheinland-Pfalz: *Statistisches Jahrbuch 2014*, 2014.
- 347 Strahler, A. N.: Quantitative analysis of watershed geomorphology, *Eos, Transactions American Geophysical*  
 348 *Union*, 38, 913-920, 1957.
- 349 Stumm, W., and Morgan, J. J.: *Aquatic chemistry: chemical equilibria and rates in natural waters*, Wiley, 1996.
- 350 Tranvik, L. J., Downing, J. A., Cotner, J. B., Loiselle, S. A., Striegl, R. G., Ballatore, T. J., Dillon, P., Finlay, K.,  
 351 Fortino, K., Knoll, L. B., Kortelainen, P. L., Kutser, T., Larsen, S., Laurion, I., Leech, D. M., McCallister, S. L.,  
 352 McKnight, D. M., Melack, J. M., Overholt, E., Porter, J. A., Prairie, Y., Renwick, W. H., Roland, F., Sherman, B.  
 353 S., Schindler, D. W., Sobek, S., Tremblay, A., Vanni, M. J., Verschoor, A. M., von Wachenfeldt, E., and  
 354 Weyhenmeyer, G. A.: Lakes and reservoirs as regulators of carbon cycling and climate, *Limnol. Oceanogr.*, 54,  
 355 2298-2314, 10.4319/lo.2009.54.6\_part\_2.2298, 2009.
- 356 Wallin, M. B., Grabs, T., Buffam, I., Laudon, H., Ågren, A., Öquist, M. G., and Bishop, K.: Evasion of CO<sub>2</sub> from  
 357 streams – The dominant component of the carbon export through the aquatic conduit in a boreal landscape, *Global*  
 358 *Change Biol.*, 19, 785-797, 10.1111/gcb.12083, 2013.
- 359 Zhao, M., Heinsch, F. A., Nemani, R. R., and Running, S. W.: Improvements of the MODIS terrestrial gross and net  
 360 primary production global data set, *Remote Sensing of Environment*, 95, 164-176, 10.1016/j.rse.2004.12.011, 2005.



361

362 **Fig. 1:** Map of the stream network (black lines) within the state borders of Rhineland Palatinate in southwest Germany.  
363 The inset map in the upper left corner indicates the location of the study region in central Europe. Filled circles mark the  
364 position of sampling sites with color indicating stream order (SO1 – SO4; the numbers in brackets in the legend are the  
365 respective number of sampling sites). The catchment areas of the sampling sites are marked in grey color.

366

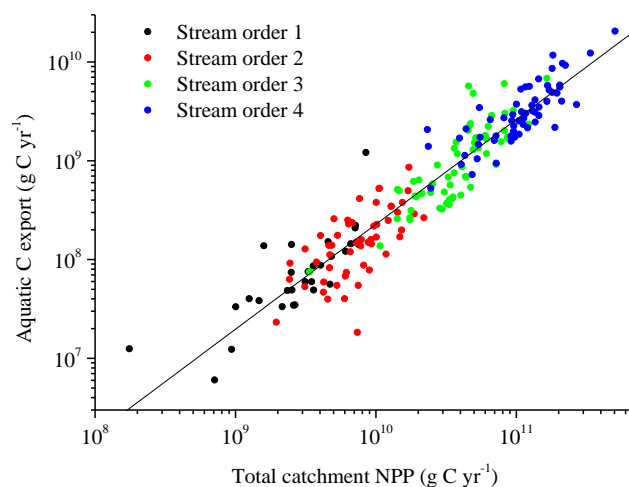


367



368 **Fig. 2: TOC concentration versus DIC concentration. Different colors indicate sampling sites from different stream**  
369 **orders. The solid line shows the fitted linear regression model with  $\text{TOC}=0.04 \cdot \text{DIC}$  ( $r^2=0.33, p<0.001$ ).**

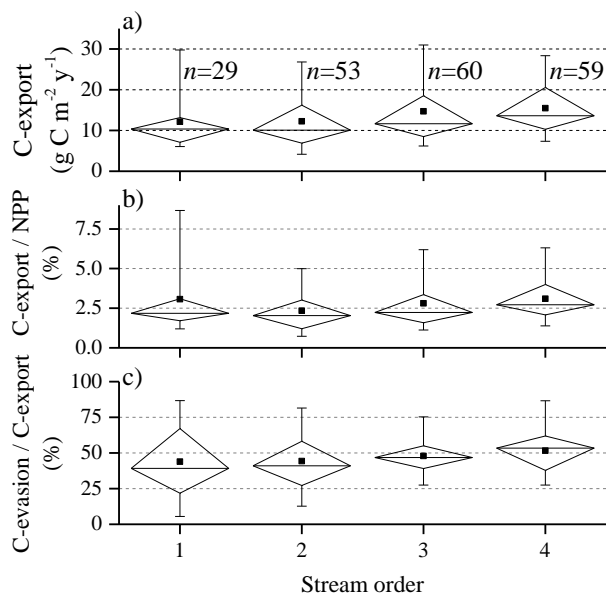
370



371

372 **Fig. 3: Annual rate of C export through the stream network versus terrestrial NPP in the catchment area. Different colors**  
373 **indicate sampling sites from different stream orders. The solid line shows the fitted linear regression model for the log-**  
374 **transformed data with  $C_{\text{export}}=0.005 \cdot \text{NPP}^{1.06}$  ( $r^2=0.89, p<0.001$ ).**

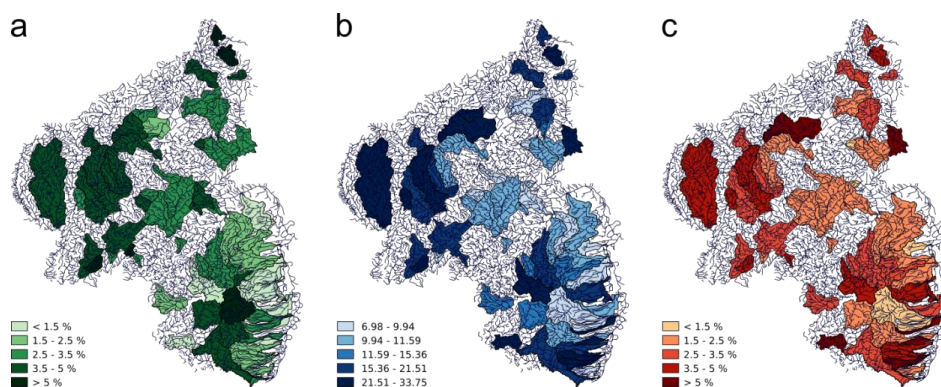
375



376

377 **Fig. 4:** a) Boxplots of C export (sum of evasion and discharge) normalized by catchment area. b) Boxplots of the ratio of  
 378 the total exported C and terrestrial NPP for different stream orders. c) Boxplots of the fraction of the total exported C  
 379 which is emitted to the atmosphere from the stream network for each stream order. The boxes demarcate the 25th and  
 380 75th percentiles, the whiskers demarcate the 95% confidence intervals. Median and mean values are marked as  
 381 horizontal lines and square symbols, respectively. The sample numbers (*n*) provided in a) apply to all panels.

382



383

384 **Fig. 5:** Map of 3rd and 4th order catchments showing a) Mean NPP ( $\text{g C m}^{-2} \text{yr}^{-1}$ ), b) aquatic export ( $\text{g C m}^{-2} \text{yr}^{-1}$ ), c) ratio  
 385 aquatic export/NPP (%).

386



387 **Table 1: Major hydrological characteristics,  $p\text{CO}_2$ , DIC and DOC concentrations averaged over stream orders (SO) and**  
 388 **for all sampling sites (total). All values are provided as mean $\pm$ sd (standard deviation) of the annual mean observations,  $n$**   
 389 **is the number of observations.**

	SO 1	SO 2	SO 3	SO 4	Total
$n$	29	53	60	59	201
Catchment size ( $\text{km}^2$ )	9 $\pm$ 7	16 $\pm$ 9	87 $\pm$ 54	243 $\pm$ 140	103 $\pm$ 126
Water coverage (%)	0.24 $\pm$ 0.11	0.26 $\pm$ 0.09	0.36 $\pm$ 0.11	0.42 $\pm$ 0.13	0.33 $\pm$ 0.13
Discharge ( $\text{m}^3 \text{s}^{-1}$ )	0.06 $\pm$ 0.05	0.15 $\pm$ 0.10	0.73 $\pm$ 0.63	2.20 $\pm$ 1.95	0.91 $\pm$ 1.41
Drainage rate ( $\text{m y}^{-1}$ )	0.26 $\pm$ 0.17	0.29 $\pm$ 0.16	0.27 $\pm$ 0.17	0.30 $\pm$ 0.21	0.28 $\pm$ 0.18
$p\text{CO}_2$ (ppm)	2597 $\pm$ 1496	1819 $\pm$ 1095	1992 $\pm$ 1327	2162 $\pm$ 1302	2083 $\pm$ 1303
DIC ( $\text{g m}^{-3}$ )	38.8 $\pm$ 30.3	34.2 $\pm$ 31.1	34.6 $\pm$ 22.4	32.4 $\pm$ 21.0	34.5 $\pm$ 25.7
DOC ( $\text{g m}^{-3}$ )	3.54 $\pm$ 1.86 ( $n=5$ )	4.11 $\pm$ 0.73 ( $n=4$ )	4.17 $\pm$ 1.08 ( $n=22$ )	4.10 $\pm$ 1.24 ( $n=33$ )	4.08 $\pm$ 1.20 ( $n=64$ )

390

391 **Table 2: Aquatic C-fluxes and terrestrial NPP in catchments drained by streams of different stream orders (SO) and for**  
 392 **all sampling sites (total). All values are mean  $\pm$  standard deviation. The  $\text{CO}_2$  flux from the water surface (first row) is**  
 393 **expressed per square meter water surface area, while the remaining fluxes are expressed per square meter catchment**  
 394 **area.**





	SO 1	SO 2	SO 3	SO 4	Total
CO <sub>2</sub> flux from water surface (g C m <sup>-2</sup> yr <sup>-1</sup> )	2415±2335	1975±1364	1998±1671	1928±903	2032±1528
CO <sub>2</sub> evasion per catchment area (g C m <sup>-2</sup> yr <sup>-1</sup> )	5.9±6.3	5.2±4.1	7.0±6.6	8.0±4.6	6.6±5.5
DIC discharge per catchment area (g C m <sup>-2</sup> yr <sup>-1</sup> )	6.2±4.5	7.1±6.1	7.7±5.7	7.5±4.7	7.3±5.4
Total aquatic C export per catchment area (g C m <sup>-2</sup> yr <sup>-1</sup> )	12.1±6.9	12.3±6.9	14.7±10.8	15.5±6.7	13.9±8.3
NPP (g C m <sup>-2</sup> yr <sup>-1</sup> )	466±127	536±66	527±57	508±69	515±79

395

396 **Table 3: Summary of estimates of aquatic C export in relation to terrestrial production in the watershed across different**  
 397 **spatial scales (spatial scale decreases from top to bottom). Aquatic C export is the sum of C-discharge and evasion**  
 398 **(numbers in parentheses also include the change in C storage in the aquatic systems by sedimentation) normalized by the**  
 399 **area of the terrestrial watershed. Aquatic C fate refers to the percentage of the total exported C which is emitted to the**  
 400 **atmosphere (evasion) and transported downstream (discharge). The missing percentage is the fraction which is stored in**  
 401 **the aquatic systems by sedimentation (if considered). Terrestrial production is expressed as NPP or as net ecosystem**  
 402 **exchange (NEE). n.c. indicates that this compartment/flux was not considered in the respective study.**

Study area (Catchment size in km <sup>2</sup> )	Fractional water coverage (%) Rivers Lakes	Aquatic C export (g C m <sup>2</sup> yr <sup>-1</sup> )	Aquatic C fate (%): Evasion Discharge	Aquatic C export / terrestrial production (%)		Reference
				NPP	NEE	
Global (1.3x10 <sup>8</sup> )	R: 0.2-0.3 L: 2.1-3.4	16 (20)	E: 44 D: 34	3.7 <sup>1</sup>	21-64 <sup>2</sup>	(Aufdenkampe et al., 2011)
Conterminous U.S. (7.8x10 <sup>6</sup> )	R: 0.52 L: 1.6	13.5 (18.8)	E: 58 D: 28	3.6	27 <sup>3</sup>	(Butman et al., 2015)
Central Amazon (1.8x10 <sup>6</sup> )	4-16	78	E: 87 D: 13	6.8 <sup>4</sup>	n.c.	(Richey et al., 2002)
Yellow River network (7.5x10 <sup>5</sup> )	R: 0.3-0.4 L: n.c.	18.5 (30)	E: 35 D: 26	n.c.	96 (62)	(Ran et al., 2015)
North temperate lake district (6400)	R: 0.5 L: 13	11.8 (16)	E: 33 D: 41	n.c.	7	(Buffam et al., 2011)



Northern Sweden (peat) (3025)	R: 0.33 L: 3.5	9	E: 50 (4.5) D: 50 (4.5)	n.c.	6	(Jonsson et al., 2007)
<b>Temperate streams (0.7- 1227)</b>	<b>R: 0.33 L: n.c.</b>	<b>13.9</b>	E: 47 D: 53	<b>2.7</b>	n.c.	<b>This study</b>
English Lake district (1 - 360)	R: n.c. L: 2.2	5.4	E: 100 D: n.c.	1.6	n.c.	(Maberly et al., 2013)
Forested stream catchments in Sweden (0.46 - 67)	R: 0.1-0.7 L:n.c. (<0.7)	9.4	E: 53 D: 47	n.c.	8-17	(Wallin et al., 2013)
Forest catchment in Japan (9.4)	R: - L: n.c.	4	E: n.c. D: 100	n.c.	2	(Shibata et al., 2005)
Peatland catchment (3.35)	R: 0.05 L: n.c.	30.4	E: 13 D: 87	n.c.	160	(Billett et al., 2004)
Peatland catchment (2.7)	R: n.c. L: 2.2	12.2	E: - D: -	n.c.	12-50	(Leach et al., 2016)

403 <sup>1</sup> For a value of 56 Pg C yr<sup>-1</sup> for global NPP (Zhao et al., 2005).

404 <sup>2</sup> Global mean NEE was estimated as the difference of GPP and ecosystem respiration, which was assumed to be 91-  
405 97 % of GPP (Randerson et al., 2002).

406 <sup>3</sup> This percentage refers to NEP instead of NEE.

407 <sup>4</sup> For a global mean value of NPP in tropical forests of 1148 g C m<sup>2</sup> yr<sup>-1</sup> (Sabine et al., 2004).

408